HHS Public Access

Author manuscript

Optica. Author manuscript; available in PMC 2017 October 16.

Published in final edited form as:

Optica. 2017 ; 4(2): 222–228. doi:10.1364/OPTICA.4.000222.

Whispering-gallery-mode emission from biological luminescent protein microcavity assemblies

Matjaž Humar[1,2,3] and **Seok Hyun Yun**[1,4,*]

[1]Wellman Center for Photomedicine, Harvard Medical School, Massachusetts General Hospital, 65 Landsdowne St. UP-5, Cambridge, Massachusetts 02139, USA

[2]Condensed Matter Department, J. Stefan Institute, Jamova 39, SI-1000 Ljubljana, Slovenia

[3]Faculty of Mathematics and Physics, University of Ljubljana, Jadranska 19, SI-1000, Ljubljana, Slovenia

[4]Harvard-MIT Health Sciences and Technology, Cambridge, 77 Massachusetts Avenue Cambridge, Massachusetts 02139, USA

Abstract

Fluorescence and bioluminescence are widely used to study biological systems from molecular to whole organism level. However, their broadband emission is often a bottleneck for sensitive spectral measurements and multiplexing. To overcome the limitation, the emitters can be coupled with optical cavity modes to generate narrowband spectral features. Here we demonstrate several types of emitter-resonator complexes made of fluorescent or bioluminescent proteins and artificially or naturally formed optical resonators. We engineered cells to express green fluorescent protein (GFP) fused with ABHD5, which binds to oil or lipid droplets supporting whispering gallery modes (WGM). The genetically-integrated complexes feature well-defined WGM spectral peaks. We measured WGM peaks from GFP-coated $BaTiO_3$ beads (2.56 μm in diameter) during mitosis. Finally, we demonstrate cavity-enhanced bioluminescence using luciferase-coated beads and biochemical excitation. The ability to tailor spontaneous emission by cavity resonance inside biological systems should have applications in biological sensing, imaging and cell tagging.

1. INTRODUCTION

Lasers are widely used for biomedical applications, providing photons for sensing and imaging and delivering optical energy for photothermal and photochemical effects. While the lasers today are built on inanimate engineered materials and mostly in macroscopic sizes, efforts have recently begun to redesign lasers with biocompatible materials and microscopic scales so that they are more seamlessly integrated with the biological systems. At the heart of this new initiative is a biological laser where all three basic elements of the laser—namely gain medium, resonator, and pump energy—are provided by biological systems themselves. One of the first steps in this endeavor was the demonstration of protein lasers, where

*Corresponding author: syun@hms.harvard.edu.

See Supplement 1 for supporting content.

fluorescent proteins in cells allowed lasing [1–4]and optical amplification [5,6]. The genetically produced gain medium provides means to connect the optical properties of the laser with the genetic and functional phenotypes of the host cell. All the previous protein lasers, however, used external resonators, such as mirrors, placed outside cells. Another major advance in the quest of biological lasers was the recent demonstration of intracellular lasers, made possible by using micron-sized spheres made of organic polymers or oil droplets, in conjunction with organic dyes as the gain materials [7–9]. Besides the unique characteristics of lasing and stimulated emission, the coupling of the luminescent molecules with optical resonators can alter spontaneous emission kinetics due to wavelength-dependent changes in the optical density of states. This interaction results in emission characteristics distinctly different from the materials' intrinsic luminescence even at pumping levels below lasing threshold. At the resonant wavelengths of the cavity, spontaneous emission rates are increased through the emitter-cavity interaction known as the Purcell effect [10], and the emission exhibits narrow spectral features that are enhanced by the optical resonant modes of the cavity [11]. Because of their small mode volumes and high Q-factors, WGM cavities are especially efficient in exhibiting cavity enhanced fluorescence. The effect has been widely studied theoretically and experimentally in solid [12] and droplet [13–15] WGM cavities.

Here, we present steps toward all-biological gain medium, resonator, and pumping by demonstrating several different embodiments of protein-cavity assemblies capable of generating spontaneous emission with narrowband spectral features. First, we demonstrate recombinant GFP-beads in cells, which exhibit distinct WGM features. Second, we build a cellular system based on genetically modified adipocytes, which makes both a gain medium and a resonator genetically integrated and produced by self-assembly. Finally, we integrate cavity resonance and bioluminescence to realize WGM-modified emission driven by chemical energy, without the need of any external light source for optical pumping.

2. RESULTS

A. GFP coated beads *in vitro*

We have prepared $BaTiO_3$ glass beads (n = 1.95) coated with GFP. Polydisperse $BaTiO_3$ beads with a size distribution of 1–40 μm (GL0175B, Mo-Sci) were used. Eukaryotic cells can spontaneously internalize microbeads with diameters up to a considerable fraction of the cell size, via endocytosis. The beads were washed once with acetone, centrifuged at 5,000 g for 5 min and re-dispersed in acetone containing 2% v/v 3-aminopropyltriethoxysilane (APTES) for 15 min with mixing. The beads were washed twice with acetone and then washed with water and dried at 120 °C for 30 min. The beads were incubated in 10% solution of glutaraldehyde for 1 h. The beads were washed three times with water and re-dispersed in 27 μM GFP solution in phosphate-buffered saline (PBS, pH 7.4). After mixing for 2 h, the beads were washed five times with PBS using centrifugation. This protocol produced GFP-coated $BaTiO_3$ beads. For *in situ* real-time measurement of GFP binding, $BaTiO_3$ beads after incubation with glutaraldehyde were added into a 14-nM GFP solution prepared by adding 10 μl of 0.27 μM GFP solution in 200 μl medium (PBS), so that the

amine-reactive surface of the beads accumulated free-floating GFP molecules over time (Fig. 1a).

An inverted microscope setup coupled with pump light sources and a spectrometer was used to study the GFP coated beads (Fig. S1). For illumination of GFP and collection of fluorescence, a 100× 1.40 NA or 40× 1.25 NA oil immersion objectives (Olympus) were used. Either a continuous-wave 491-nm laser (Cobolt Dual Calypso) or a 455-nm light-emitting diode (LED) (Thorlabs) with a bandpass filter centered at 469 nm and FWHM of 35 nm was used. Both light sources produced similar results. The collected light was sent through a dichroic mirror (edge at 500 nm) and split 50:50 to camera (Luca, Andor) and imaging spectrometer (300 mm focal length, 0.05 nm resolution, Andor).

For intracellular operation, the GFP-coated $BaTiO_3$ beads were incubated with and internalized into HeLa cells in culture. HeLa cells (ATCC) were grown at 37 °C with 5% CO_2 in full growth medium (Dulbecco's Modified Eagle Medium supplemented with 10% fetal bovine serum and 1% pen-strep), and they were incubated in full growth medium supplied with GFP coated beads for 12 h prior to optical measurements with pumping by blue LED light. The fluorescence from the cells with intracellular beads exhibited typical WGM spectra (Fig. S2). Cells were viable over a few days; the maximum period we have monitored. During this period, we observed cellular division, after which the bead in the parent cell is passed on to one of the two daughter cells (Fig. 2a). We observed dynamic changes of WGM resonance wavelengths by typically 20–30 pm during cytokinesis (Fig. 2b). This tiny, but measurable, modal shift is due to the change in the bead's surrounding environment, which affects the effective refractive index of the WGMs.

B. *In situ* assembly of GFP gain on to injected oil droplets

We have previously achieved intracellular lasing by injecting dye-doped polyphenyl ether oil (n = 1.69) into the cytosol to form a micro-droplet laser [8]. To demonstrate *in-vitro* gain formation, we designed a cellular system based on oil droplets and lipid-binding GFP fusion proteins. We chose α/β hydrolase domain-containing protein 5 (ABHD5), which is known to play roles in intracellular phospholipid metabolism and localize on the surface of lipid droplets [17,18]. For expression of GFP fused to abhydrolase domain containing 5 (ABHD5, CGI-58), a plasmid was engineered (pLV[Exp]-EF1A>EGFP:mAbhd5[ORF037106], Cyagen), (Fig. S3). For transduction, the vector was delivered to adipocytes or HeLa cells by HIV-1-derived lentivirus (Cyagen) with titer concentration of $(3.31 \pm 2) \times 10^9$ TU/mL, at multiplicity of infection (MOI) of 50 with an addition of 8 μg/ml hexadimethrine bromide (Polybrene, Cyagen) and incubated for 48 h. The cells were washed with fresh medium and incubated for additional 4 days before the optical measurements. Transduction of HeLa cells with a lentiviral vector encoding GFP-ABHD5 gene resulted in bright GFP fluorescence with relatively uniform intensity throughout the cytoplasm.

The GFP-transduced HeLa cells were injected with a non-toxic, low-viscosity high-index polyphenyl ether oil (PPE, SL-5267, Santolubes). The injection was performed using a microinjector (FemtoJet, Eppendorf) and a glass micropipette with 1.0 μm outer diameter (Femtotip, Eppendorf). The size of the injected droplets was controlled by the injection time ranging from 0.2 to 1 s, with an injecting pressure of 1,700 kPa. Upon injection of un-doped

PPE oil by using a micropipette (Fig. 3a), within less than one hour an apparent accumulation of GFP on the surface of the droplets was observed under fluorescence microscopy (Fig. 3b). The output spectrum from a single cell when illuminated with a CW laser light (491 nm) showed typical WGM spectral peaks (Fig. 3c). We intentionally photobleached the GFP in the cells (Fig. 3d) by extensive exposure with high-intensity CW light for 10 s. Within 6 hours after photo-bleaching, we observed partial, yet significant, recovery of fluorescence brightness both in the cytosol and on the surface of oil droplets (Fig. 3e). This experiment demonstrates the self-healing nature of the genetically integrated, self-assembled gain medium.

C. Self-assembled gain and resonator in adipocyte cells

To realize both biologically formed gain medium as well as optical cavity inside a cell, we transduced 3T3-L1 cells, fully differentiated to form large lipid droplets, with a GFP-ABHD5 lentiviral vector (Fig. 4a). 3T3-L1 preadipocytes (ATCC) were grown in glass bottom 96-well plates at 37 °C with 5% CO_2. The preadipocyte medium (ZenBio) was changed every two days until the cells were confluent. Once confluent, the cells were incubated an additional 48 hours, after which the medium was exchanged with differentiation medium (ZenBio). After 3 days the medium was replaced by adipocyte maintenance medium (ZenBio), and the medium was exchanged every 3 days for 4 weeks. The adipocytes were then transduced in the same way as HeLa cells and incubated for additional 4 days before the optical measurements.

The GFP-ABHD5 fusion protein was found to locate at higher concentrations around the lipid droplets, as apparent from bright fluorescent rings (Fig. 4b). The binding mechanism, although not fully understood [19], should involve perilipin, a protein that coats lipid droplets and protects them from lipases. The emission spectrum from a single droplet pumped by CW blue laser light (491 nm) showed weak, yet well defined, periodic mode structure at a spacing corresponding to the droplet diameter, superimposed on typical broadband GFP-fluorescence (Fig 4c). The WGM peaks were less prominent above the broadband fluorescence because they are wider, with lower Q-factor. The measured Q-factor was 460, lower than the theoretical radiation-loss-limited Q-factor of 4,300 for a droplet of the size (22 μm). This discrepancy is reasonable considering the possible un-resolvable mode splitting due to droplet deformation [20] and possibly scattering loss at contacts with other smaller lipid droplets in the cytoplasm. In contrast to the GFP-ABHD5-transduced cells, GFP-transduced 3T3-L1 cells showed uniformly dispersed GFP molecules in the cytosol and failed to produce any noticeable cavity-modified spectral feature in fluorescence (Fig. S4).

We illuminated the droplet of a GFP-ABHD5-transduced adipocyte with high-intensity blue laser light (300 μW) for 200 s to induce bleaching of the GFP, causing the significant reduction of both fluorescence background and WGM structure (Fig. S5). After incubation in the dark for 18 h, the same cell exhibited partial recovery of the fluorescence intensity at the same pumping condition (Fig. 4d). This experiment demonstrates as well the remarkable self-healing capability of the biologically formed, gain-resonator system.

The Q-factors of intrinsic lipid droplets are not typically sufficient for practical applications to cell tagging and multiplexed imaging, although they may be used for mechanical force sensing via deformation-induced spectral broadening [21]. The size of lipid droplets can change over time as the cells accumulate or consume lipids, possibly enabling precise measurement of adipocyte metabolism.

D. Bioluminescence pumped WGMs

Bioluminescence produces a photon as a product of chemical reaction of luciferin, a substrate, and luciferase, an enzyme that catalyses the reaction [22]. To our knowledge, the cavity-enhanced Purcell effect in bioluminescence, or more generally chemiluminescence, has not been demonstrated before. To explore a biochemical energy-driven gain/resonator system, we used biotinylated *Gaussia* luciferase (GLuc, 19.9 kDa) [23] and conjugated the bioluminescence enzymes onto the streptavidin-coated surface of polystyrene micro-beads. SuperAvidin™-coated polystyrene microspheres with mean diameter of 9.95 μm (Bangs Laboratories) were used. The beads were washed twice with Tris buffer (pH 7.8). For conjugation, 2 mg of beads were dispersed in 100 μl of 100 μg/ml biotinylated luciferase and incubated at room temperature for 1 h. Luciferase from *Gaussia* princeps (GLuc, NanoLight) contained biotin covalently attached to the lysine in the Avitag peptide (GLNDIFEAQKIEWHE, C-terminus). This streptavidin-biotin binding system is more effective than nonspecific amine-reactive chemicals, such as glutaraldehyde, which can reduce the activity of luciferase by reacting with the amino groups at the active site [24]. The beads were afterward washed five times with Tris buffer and transferred to PBS. Bioluminescence was initiated by adding 5 μl of 500 μM water-soluble native coelenterazine (CTZ, Nanolight) in PBS to 100 μg of beads in 95 μl of PBS, producing a final CTZ concentration of 25 μM. For optical measurements, the light source was not used and the dichroic was removed. Instead of beam splitter a removable mirror was used to direct all the light to either the camera or spectrometer. The spectrometer slit was open to 50 μm, compared to 15 μm used for fluorescence measurements, to gather more light. The GLuc on the bead's surface oxidizes coelenterazine (CTZ, 423.46 Da) to generate bioluminescence light, which is evanescently coupled to the WGMs in the bead (Fig 5a). A single avidin-coated bead has the capacity to bind 7.9×10^7 biotinylated luciferase molecules (manufacturer data). Since each luciferase typically produces [25] ~ 0.2 photons/s, one bead produces a peak power of ~ 1.74×10^6 photons/s or 0.72 pW. When we added CTZ (25 μM) to a medium containing dispersed GLuc-coated beads, bright bioluminescence emission was generated exclusively from the beads' surfaces (Fig. 5b). The bioluminescence intensity reached the maximum typically in 20–40 s and decayed exponentially (Fig. S6). A representative output spectrum acquired from 23 to 28 s after the addition of CTZ shows a well distinguishable WGM structure (Fig. 5c). Compared to the GFP-beads (Fig. 1), the Q-factor and peak-to-background contrast are lower. This is partly due to different spectrometer settings, where the entrance slit was opened larger (50 μm) to collect weak bioluminescence more efficiently at the sacrifice of spectral resolution (0.5 nm). A best curve-fit to the spectrum predicted an effective bead diameter of 9.378 μm, in a reasonable agreement with the manufacturer's specified mean diameter of 9.95 μm (Fig. 4d). Despite the time-dependent variation of the bioluminescence intensity, the spectral fitting of the WGMs yielded accurate measurement of the bead diameter, with a standard deviation error

of only ± 1.8 nm during a 100-s-long measurement (Fig. 5d). Such high precision may enable to use bioluminescence-cavity complexes for tagging and sensing in the same way as fluorescent cavities [8], but without the need of an external source of light.

3. DISCUSSION AND CONCLUSION

We have demonstrated several schemes to generate cavity-modified luminescence from biological systems by coupling fluorescent proteins and bioluminescence enzymes with micro-resonators. The building blocks, apart from beads and oils, were genetically integrated and self-assembled in the cytoplasm. The fine spectral features of cavity-tailorable WGMs are suitable for tagging and sensing, adding extra dimension to broadband spectra of fluorescence and bioluminescence. All the demonstrations herein describe spontaneous emission at relatively low pumping levels. Stimulated emission and lasing may be possible with nanosecond optical pumping, sufficient amount of gain molecules and high enough Q-factor, particularly from GFP-accumulated beads [5]. The use of gain material produced by the cells in the form of fluorescent proteins has several advantages over externally supplied fluorescent dyes. Namely, fluorescent proteins are continuously producible and replenished in the cells, which leads to unique self-healing capability. Further, only specific cells with certain phenotypes can be chosen to express the gain, so only those cells of interest that generate the desired emission can be studied and tracked. In contrast to the genetically-integrated elements, artificial resonators such as glass beads and oil droplets, require spontaneous cellular uptake or injection. The GFP-coated $BaTiO_3$ beads with a diameter of 2.56 μm represents the smallest WGM emitters achieved inside cells. The small sizes could facilitate the internalization of several beads into a single cell for multiplexed sensing and tagging without substantially disturbing the cell's biological functions. Besides lipid droplets, other types of resonator structures may be devised using various optical [26,27] and plasmonic elements [28] that could be genetically encoded and self-assembled [29,30] inside cells and organisms. The luciferase-cavity constructs have advantages in that they do not require external optical pumping, activated simply by injecting substrate (luciferin) molecules, and have very low background. Moreover, the bioluminescence proteins can be genetically encoded [31] to specific cells. The bioluminescence-cavity complexes can be useful for cellular sensing, tagging, and, possibly, photodynamic therapy [32], particularly in tissues at depths not reachable by external optical excitation.

Supplementary Material

Refer to Web version on PubMed Central for supplementary material.

Acknowledgments

Funding. U.S. National Institutes of Health (P41-EB015903, R01 CA192878), National Science Foundation (ECCS-1505569), Human Frontier Science Program (RGP0034/2016), MGH Research Scholar award program and 7th European Community Framework Programme (Marie Curie International Outgoing Fellowship, 627274).

References

1. Gather MC, Yun SH. Single-cell biological lasers. Nat Photonics. 2011; 5:406–410.

2. Gather MC, Yun SH. Lasing from Escherichia coli bacteria genetically programmed to express green fluorescent protein. Opt Lett. 2011; 36:3299–3301. [PubMed: 21847240]
3. Jonas A, Kiraz A, Jonáš A, Aas M, Karadag Y, Manioğlu S, Anand S, McGloin D, Bayraktar H, Kiraz A. In vitro and in vivo biolasing of fluorescent proteins suspended in liquid microdroplet cavities. Lab Chip. 2014; 14:3093–3100. [PubMed: 24968888]
4. Nizamoglu S, Gather MC, Yun SH. All-biomaterial laser using vitamin and biopolymers. Adv Mater. 2013; 25:5943–5947. [PubMed: 24425626]
5. Chen Q, Ritt M, Sivaramakrishnan S, Sun Y, Fan X. Optofluidic lasers with a single molecular layer of gain. Lab Chip. 2014; 14:4590–4595. [PubMed: 25312306]
6. Gather MC, Yun SH. Bio-optimized energy transfer in densely packed fluorescent protein enables near-maximal luminescence and solid-state lasers. Nat Commun. 2014; 5:5722. [PubMed: 25483850]
7. Himmelhaus M, Francois A. In-vitro sensing of biomechanical forces in live cells by a whispering gallery mode biosensor. Biosens Bioelectron. 2009; 25:418–27. [PubMed: 19699629]
8. Humar M, Hyun Yun S. Intracellular microlasers. Nat Photonics. 2015; 9:572–576. [PubMed: 26417383]
9. Schubert M, Steude A, Liehm P, Kronenberg NM, Karl M, Campbell EC, Powis SJ, Gather M. Lasing within live cells containing intracellular optical micro-resonators for barcode-type cell tagging and tracking. Nano Lett. 2015; 15:5647–5652. [PubMed: 26186167]
10. Purcell EM. Spontaneous emission probabilities at radio frequencies. Phys Rev. 1946; 69:681.
11. Gayral B. Controlling spontaneous emission dynamics in semiconductor micro cavities. Ann Phys (Paris). 2001; 26:1–135.
12. Benner RE, Barber PW, Owen JF, Chang RK. Observation of structure resonances in the fluorescence-spectra from microspheres. Phys Rev Lett. 1980; 44:475–478.
13. Campillo AJ, Eversole JD, Lin HB. Cavity quantum electrodynamic enhancement of stimulated emission in microdroplets. Phys Rev Lett. 1991; 67:437–440. [PubMed: 10044894]
14. Holler S, Goddard NL, Arnold S. Spontaneous emission spectra from microdroplets. J Chem Phys. 1998; 108
15. Arnold S. Cavity-enhanced fluorescence decay rates from microdroplets. J Chem Phys. 1997; 106:8280–8282.
16. Gorodetsky ML, Fomin AE. Geometrical theory of whispering-gallery modes. Sel Top Quantum Electron IEEE J. 2006; 12:33–39.
17. Subramanian V, Rothenberg A, Gomez C, Cohen AW, Garcia A, Bhattacharyya S, Shapiro L, Dolios G, Wang R, Lisanti MP, Brasaemle DL, Rotlienberg A, Gomez C, Cohen AW, Garcia A, Bhattacharyya S, Shapiro L, Dolios G, Wang R, Lisanti MP, Brasaemle DL. Perilipin A mediates the reversible binding of CGI-58 to lipid droplets in 3T3-L1 adipocytes. J Biol Chem. 2004; 279:42062–42071. [PubMed: 15292255]
18. Yamaguchi T, Omatsu N, Matsushita S, Osumi T. CGI-58 interacts with perilipin and is localized to lipid droplets. Possible involvement of CGI-58 mislocalization in Chanarin-Dorfman syndrome. J Biol Chem. 2004; 279:30490–30497. [PubMed: 15136565]
19. Thiam AR, Farese RV Jr, Walther TC. The biophysics and cell biology of lipid droplets. Nat Rev Mol cell Biol. 2013; 14:775–786. [PubMed: 24220094]
20. Riesen N, Reynolds T, François A, Henderson MR, Monro TM. Q-factor limits for far-field detection of whispering gallery modes in active microspheres. Opt Express. 2015; 23:28896. [PubMed: 26561158]
21. Himmelhaus M, Francois A. In-vitro sensing of biomechanical forces in live cells by a whispering gallery mode biosensor. Biosens Bioelectron. 2009; 25:418–427. [PubMed: 19699629]
22. Contag CH, Bachmann MH. Advances in in vivo bioluminescence imaging of gene expression. Annu Rev Biomed Eng. 2002; 4:235–260. [PubMed: 12117758]
23. Kay, B., Thai, S., Volgina, V. High-throughput biotinylation of proteins. High Throughput Protein Expression and Purification SE - 13. In: Doyle, S., editor. Methods in Molecular Biology. Vol. 498. Humana Press; 2009. p. 185-198.

24. Ribeiro AR, Santos RM, Rosário LM, Gil MH. Immobilization of luciferase from a firefly lantern extract on glass strips as an alternative strategy for luminescent detection of ATP. J Biolumin Chemilumin. 1998; 13:371–378. [PubMed: 9926365]
25. Loening AM, Wu AM, Gambhir SS. Red-shifted Renilla reniformis luciferase variants for imaging in living subjects. Nat Methods. 2007; 4:641–643. [PubMed: 17618292]
26. Humar M, Kwok SJJ, Choi M, Cho S, Yetisen AK, Yun SH. Towards biomaterial-based implantable photonic devices. Nanophotonics. 2016; 5:60–80.
27. Kramer RM, Crookes-Goodson WJ, Naik RR. The self-organizing properties of squid reflectin protein. Nat Mater. 2007; 6:533–538. [PubMed: 17546036]
28. Fan JA, Wu C, Bao K, Bao J, Bardhan R, Halas NJ, Manoharan VN, Nordlander P, Shvets G, Capasso F. Self-assembled plasmonic nanoparticle clusters. Science. 2010; 328:1135–1138. [PubMed: 20508125]
29. Rothemund PWK. Folding DNA to create nanoscale shapes and patterns. Nature. 2006; 440:297–302. [PubMed: 16541064]
30. Rogers WB, Shih WM, Manoharan VN. Using DNA to program the self-assembly of colloidal nanoparticles and microparticles. Nat Rev Mater. 2016; 1:16008.
31. Hall MP, Unch J, Binkowski BF, Valley MP, Butler BL, Wood MG, Otto P, Zimmerman K, Vidugiris G, MacHleidt T, Robers MB, Benink Ha, Eggers CT, Slater MR, Meisenheimer PL, Klaubert DH, Fan F, Encell LP, Wood KV. Engineered luciferase reporter from a deep sea shrimp utilizing a novel imidazopyrazinone substrate. ACS Chem Biol. 2012; 7:1848–1857. [PubMed: 22894855]
32. Kim YR, Kim S, Choi JW, Choi SY, Lee SH, Kim H, Hahn SK, Koh GY, Yun SH. Bioluminescence-activated deep-tissue photodynamic therapy of cancer. Theranostics. 2015; 5:805–817. [PubMed: 26000054]

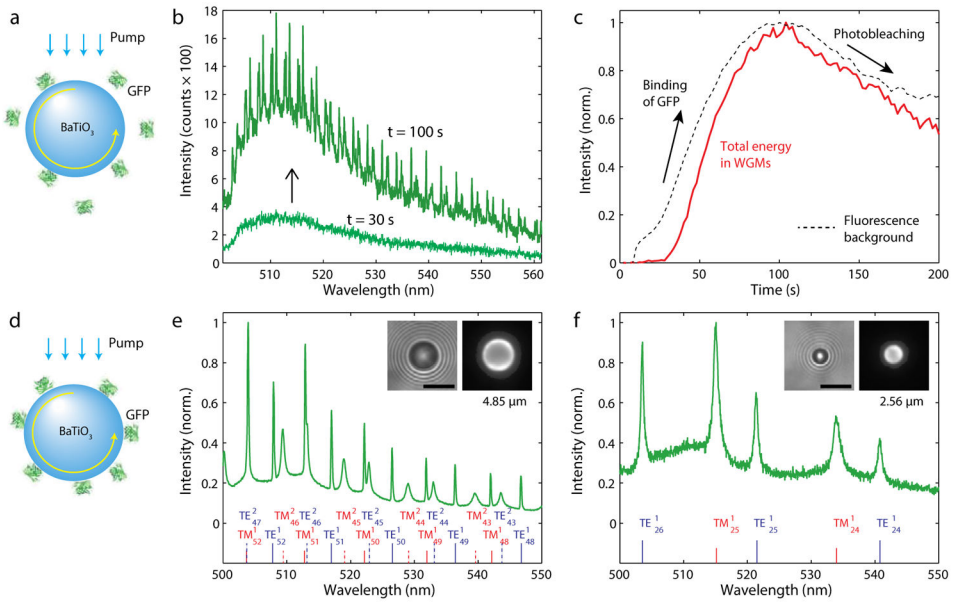

Fig. 1.

GFP on high-index microspheres. (a) Illustration of GFP molecules binding onto the surface of a $BaTiO_3$ bead. (b) Fluorescence spectra measured at 30 s and 100 s, respectively, after adding a GFP solution to beads in dispersion. (c) Intensity of the WGM peaks and background fluorescence after the addition of GFP. (d) A $BaTiO_3$ glass bead coated with GFP molecules. The fluorescent light from the GFP molecules is coupled into WGMs. (e) Fluorescence spectrum of a $BaTiO_3$ bead. Curve fitting indicates the oscillation of the first and second-order radial modes (marked) and predicts a bead diameter of 4.85 μm. Insets show bright-field (left) and fluorescence (right) images of the bead. (f) The output spectrum from a 2.56-μm bead, shows the excitation of only the first-order radial modes. Scale bars, 5 μm.

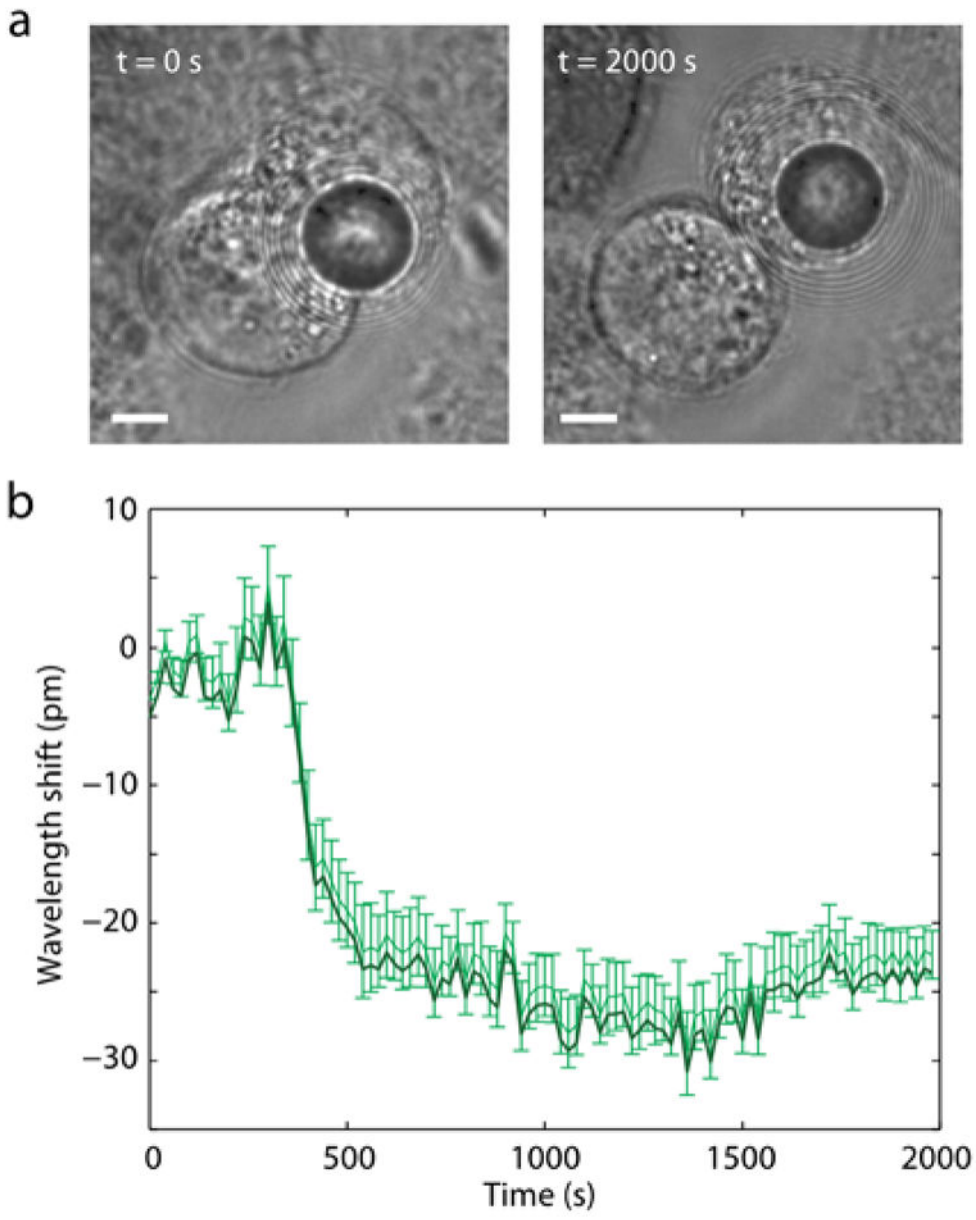

Fig. 2.

An intracellular GFP-coated glass bead during cell division. (a) Bright-field images showing the transmission of the bead during telophase (t=0 s) and after cytokinesis (t=2000 s). Scale bars, 5 μm. (b) Measured spectral shifts of the WGM peaks from telophase to the completion of mitosis.

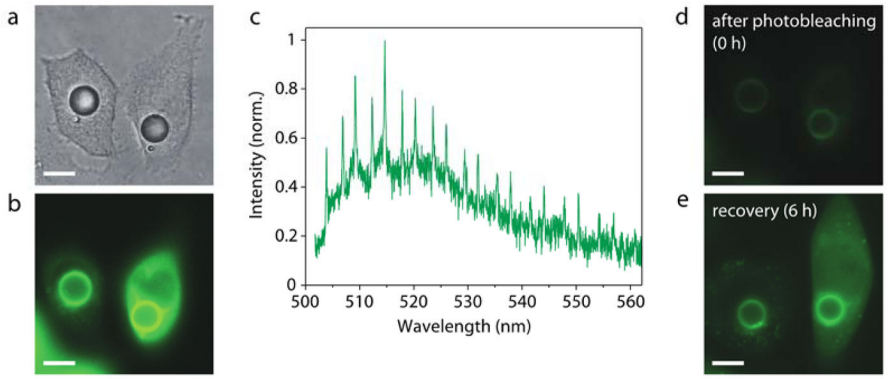

Fig. 3.

Micro-cavities in cells with GFP gain formed *in situ*. (a) Bright-field image of two GFP-ABHD5 producing HeLa cells 2 days after injecting PPE oil droplets into the cytosol. (b) Fluorescence image of the cells, showing bright green fluorescence from the accumulated GFP on the surface of the droplets. (c) Typical output spectrum from the cell under continuous-wave pumping. (d) Reduced fluorescence emission after photobleaching by high-intensity optical pumping. (e) Increased fluorescence by continuous production and replenishment of GFP *in vitro* over 6 h after the bleaching. Scale bars, 10 μm.

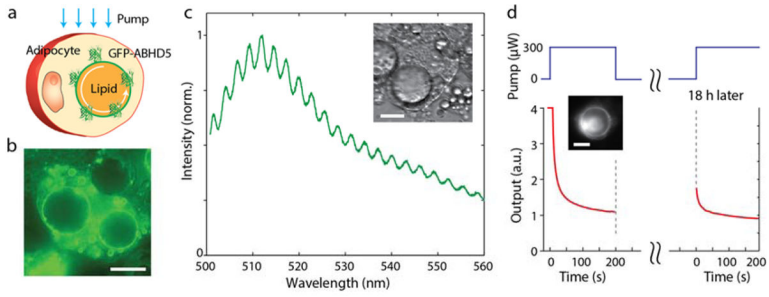

Fig. 4.

An all-biological self-assembled micro-cavity. (a) Schematic of the intracellular GFP-droplet system. (b) Fluorescence image of GFP-ABHD5-transduced 3T3-L1 mature adipocytes. The fluorescence is mainly emitted from the edges of the droplets. (c) A typical output spectrum from a single GFP-bound lipid droplet (inset). (d) Time-lapse variation of the fluorescence intensity during photobleaching and after partial recovery 18 hours later. Inset, fluorescence image at t=0. Scale bars, 20 μm.

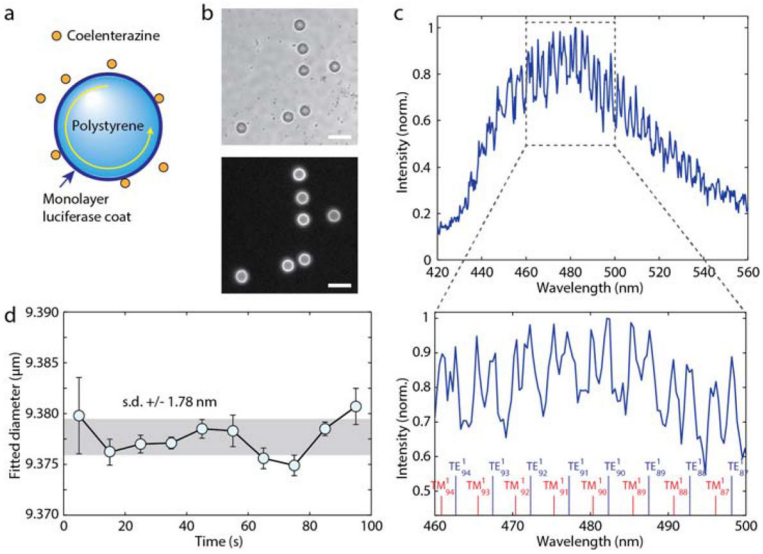

Fig. 5.

Cavity-modified bioluminescence. (a) Schematic of a polystyrene or glass bead coated with luciferase proteins. Upon addition of luciferin light is generated and coupled into WGMs. (b) Bright-field image of polystyrene beads coated with luciferase (top) and bioluminescence emission when CTZ is added (bottom). Scale bar, 20 μm. (c) A representative bioluminescence spectrum from a luciferase-coated bead. The spectral peaks of WGMs are fitted to theory to determine the mode orders and bead diameter. (d) The effective bead diameter measured over time. The standard deviation fluctuation (gray area) is ~190 ppm.